

## Improved segmentation of mouse MRI data using multiple automatically generated templates

M. M. Chakravarty<sup>1,2</sup>, M. C. van Eede<sup>1</sup>, and J. P. Lerch<sup>1</sup>

<sup>1</sup>Mouse Imaging Centre (MICE), The Hospital for Sick Children, Toronto, Ontario, Canada, <sup>2</sup>Rotman Research Institute, Baycrest, Toronto, Ontario, Canada

**Introduction:** Structural magnetic resonance imaging (MRI)-based atlases have long been used to automatically segment neuroanatomical structures. In its simplest form, this technique requires that anatomical regions be manually identified on a single high-resolution, high-contrast MRI atlas by an expert manual rater [1,2,3]. This atlas can then be customized to the anatomy of another subject by estimating a nonlinear transformation that matches the subject's neuroanatomy to the neuroanatomy of the template. This transformation is then applied to the anatomical labels in order to finish the customization process. In human MRI experiments, the accuracy of this technique is limited by errors in the nonlinear transformation estimated, differences in the neuroanatomy (such as varying gyrification patterns) between the template brain and the subject, or label resampling errors. Recent work demonstrates improvement of these segmentation techniques through the use of a template library. In this methodology, instead of using a single expertly labeled MRI template, a number of different templates are manually labeled [4,5] and transformations are estimated to match a single subject to each of these templates. After the nonlinear transformations are applied to the anatomical labels, a histogram of labels generated at each voxel can be used to inform the final segmentation on a voxel-by-voxel basis. This template library approach thus improves segmentation accuracy by accounting for varying anatomy through the use of different templates and compensating for registration algorithm inaccuracy by virtue of the multiple registrations needed from each MRI in the template to the target. In the segmentation of MRI data from inbred laboratory mice strains, however, the confounds of variable neuroanatomy are limited [5], and segmentation errors therefore result from registration inaccuracy and resampling errors. We hypothesize that segmentations can be improved if resampling and nonlinear transformation errors are reduced. Here, we test this hypothesis by implementing a multi-atlas segmentation scheme using automatically generated atlases (instead of manually labeled ones) and verified the accuracy of the segmentation using manually derived gold standards of the neuroanatomy.

**Materials and Methods:** T2-weighted MRI data from 25 C57BL/6 from fixed gadolinium-enhanced post-mortem mice brain specimens were used to create multiple registration templates. Sample preparation is similar to the method described previously in our group [2,7]. A multi-channel 7.0 T MRI scanner (Varian Inc., Palo Alto, CA) with a 6-cm inner bore diameter insert gradient set was used to acquire anatomical images of brains within skulls. Prior to imaging, the samples were placed into 13-mm-diameter plastic tubes filled with a proton-free susceptibility-matching fluid (Fluorinert FC-77, 3M Corp., St. Paul, MN). Three custom-built, 14-mm-diameter solenoid coils with a length of 18.3 mm and over wound ends were used to image three brains in parallel. Parameters used in the scans were optimized for grey/white matter contrast: a T2-weighted, 3D fast spin-echo sequence, with TR/TE = 325/32 ms, four averages, field-of-view 14×14×25 mm and matrix size=432×432×780 giving an image with 32 μm isotropic voxels. Total imaging time was 11.3 h. Geometric distortion due to position of the three coils inside the magnet was corrected using an MR phantom.

**Table 1.** Parameters used for nonlinear transformation estimation.

Step size (mm)	Iterations	Gaussian Blur (mm)	Feature type
1	60	0.25	Intensity
0.5	60	0.25	Intensity
0.5	60	0.25	Gradient
0.2	10	0.25	Intensity
0.2	10	0.25	Gradient
0.1	4	None	Intensity

All values for lattice diameter were set to 1.5 x Step\_size. Regularization parameters of stiffness, weight, and similarity were set to 0.98, 0.8, and 0.8 respectively.

each voxel. The accuracy of the segmentation for both SA and MA methods was verified against manually derived "gold standard" segmentations of the hippocampus and dentate gyrus in three coronal MRI slices (all slices were approximately matched in each brain). The goodness-of-fit was estimated using the *Kappa* statistic ( $K = 2A/(2A+B+C)$ ; where *A* is the voxel common to the gold standard and the test structure and *B+C* represents the sum of the voxels uniquely identified by either the test structure or the gold standard [8]).

**Results:** The results demonstrate an improvement in the *Kappa* values for the MA method when compared to the SA method for both the hippocampus and the dentate gyrus (see Table 2). Fig 1 demonstrates a representative segmentation through the coronal plane for both SA and MA methods and demonstrates improved segmentation. In particular, there is improved structure localization and smoothing at the structure borders.

**Table 2.** Summary of *Kappa* statistic results for both single and multi-atlas methods. Values given as mean ± standard deviation (range)

Structure	Single Atlas	Multi Atlas
Hippocampus	0.91 ± 0.017 (0.87-0.93)	0.94 ± 0.012 (0.92-0.97)
Dentate Gyrus	0.88 ± 0.017 (0.84-0.91)	0.93 ± 0.021 (0.89-0.97)

All nonlinear transformations in this section were estimated using the *mni\_autoreg* software package (part of the MINC software tools), using the parameter list in Table 1. A manually created atlas with 62 anatomical structures encompassing the entire mouse brain [2] was used for the automated atlas-to-template labeling of each of these new templates. A template library was developed by estimating the nonlinear transformation that matched each of the 25 brains to the MRI-template described above using a regular single-atlas (SA) methodology (ie: subject-to-template matching). These templates were used in a multi-atlas (MA) based segmentation scheme in a leave-one-out fashion: all pair-wise nonlinear transformations were estimated (25 x 24 transformations; 600 total) and the final transformation was applied to each of the appropriate atlases. For each mouse, the final segmentation was estimated using a voting scheme, where the mode (ie: the most frequently occurring) voxel label at each location was assigned to

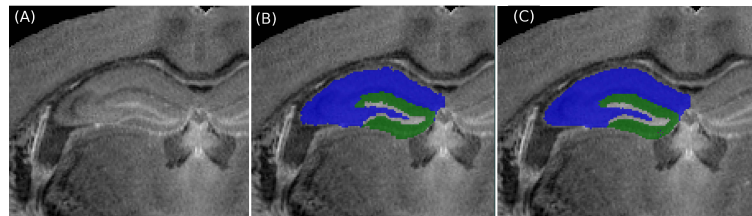


**Figure 1.** Results of SA and MA segmentations. (A) Original slice through hippocampus and dentate gyrus in one of the mouse brains used in this study. (B) + (C) SA and MA segmentations of hippocampus and dentate gyrus. The increased smoothness and boundary voxel accuracy of the MA segmentation is readily apparent.

**Conclusions:** The work presented demonstrates that segmentation of mouse MRI data can be improved by using an automatically generated multi-atlas library. The neuroanatomy in inbred mice strains is sufficiently homogenous that minimizing registration and resampling error increases the segmentation accuracy. Although the generation of a manually derived template library may be preferable, it is often difficult to find experts with sufficient expertise to engage in the painstaking work of structure identification on multiple brains. It moreover takes months to manually create a detailed brain atlas at the resolutions commonly employed in *ex vivo* mouse imaging. The real cost of our proposed technique is in the computational overhead required to achieve a single brain segmentation of an individual mouse. Given the recent advances in supercomputing infrastructures, these computational demands can be met, and represent the trade-off for improved accuracy.

**References:** [1] Kovacevic *et al.* Cerebral Cortex 15(5):639-45. [2] Dorr *et al.* NeuroImage 41(2):243-51. [3] Collins *et al.* Human Brain Mapping 3:190-208. [4] Collins and Pruessner. NeuroImage 15(4):1355-66. [5] Heckemann *et al.* NeuroImage 33(1):115-26. [6] Chen *et al.* NeuroImage 29(1):99-105. [7] Lerch *et al.* NeuroImage 32(1):32-9. [8] Chakravarty *et al.* Medical Image Analysis 12(6):873-80.